

# Dimerization Mechanism of the 1-Alkyl-4-phenylpyridinyl Radicals Generated from the Photosensitive Dimer As Studied by Kinetic ESR Spectroscopy

Kimio Akiyama, Shozo Tero-Kubota, and Yusaku Ikegami\*

Contribution from the Chemical Research Institute of Non-Aqueous Solutions, Tohoku University, Katahira 2-1-1, Sendai 980, Japan. Received September 17, 1982

**Abstract:** The dimerization mechanism of 1-methyl- (1), 1-ethyl- (2), and 1-isopropyl-4-phenylpyridinyl (3) radicals is discussed on the basis of the kinetic and thermodynamic studies. Absolute rate constants for dimerization are determined from the ESR decay curves of radicals generated by pulse photolysis of the dimer. Intermediate formation is implied by a two-step decay of the radical. The activation energy ( $E_a = 6.7$  kcal/mol) for intermediate formation is independent of the 1-alkyl group, while that for the second slow step is dependent on the alkyl group, showing  $E_a$ 's of 11.3, 12.2, and 13.3 kcal/mol for 1, 2, and 3, respectively. The equilibrium between monomeric radical and the dimer is measured and the heat of the bond formation is estimated for each radical. NMR measurement for 1 at low temperature revealed the dimer to be a 2,2'-dimer. It is proposed that the intermediate is a 4,4'-dimer which produces a 2,2'-dimer through [3,3] sigmatropic intramolecular rearrangement.

## Introduction

In our recent study,<sup>1</sup> it was revealed that 1-methyl-4-phenylpyridinyl radical (1) is isolable by distillation under vacuum and the radical is in equilibrium with the diamagnetic dimer in solution. The 2-methyltetrahydrofuran (MTHF) solution of 1 at room temperature has a greenish orange color and an ESR spectrum with well-resolved hyperfine structure (hfs) at moderate radical concentrations. At 77 K, the solution is green and shows no ESR signal because equilibrium lies in favor of the dimer at low temperature. Irradiation of the solution at 77 K with visible light resulted in a change in color to violet and an appearance of a new ESR signal due to the triplet radical pair formed by a cleavage of the dimer. This indicates that the dimer of 1 is photosensitive to visible light, as observed for the dimer of 1-methyl-2-methoxycarbonylpyridinyl.<sup>2,3</sup> The photolysis is caused by the absorption at 390 nm which is broad and spread over the visible region. At room temperature, photolysis causes an enhancement of the ESR signal of 1 and the rate of the reversible change in signal intensity is very rapid. The phenomenon is a type of photochromism, a subject of interest to many investigators.<sup>4</sup>

The purpose of this article is to present the dimerization mechanism in the dark after pulse photolysis. The kinetic ESR technique revealed the existence of a short-lived intermediate in the dimerization process. 1-Ethyl- (2) and 1-isopropyl-4-

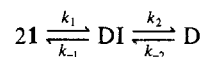
phenylpyridinyl radicals generated from the photosensitive dimer produce a 2,2'-dimer through [3,3] sigmatropic rearrangement.

## Experimental Section

The pyridinyl radicals were prepared by the reduction of the corresponding pyridinium iodides with 3% sodium amalgam in degassed acetonitrile and purified by distillation and dissolved in MTHF. Total concentration of the radical monomer and the dimer was determined by titration with 1,1'-dimethyl-4,4'-bipyridinium dichloride (methyl viologen).<sup>2</sup> The radical concentration was obtained by double integration of ESR spectrum. Diphenylpicrylhydrazyl (DPPH) in benzene ( $\epsilon = 1.415 \times 10^5$  at 519 nm) was used as standard sample. The ESR sensitivity variation was calibrated with an internal standard of strong pitch in a capillary tube. The kinetic ESR spectroscopic method has been described previously.<sup>3</sup> NMR measurement was carried out with a JEOL FT-90Q NMR spectrometer.

## Results

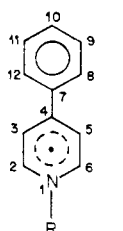
**Decay Kinetics.** Photoirradiation of the MTHF solution of 1 showed an enhancement of the ESR intensity due to the dissociation of the dimer. The change was completely reversible for the irradiation with the light of wavelengths longer than 400 nm, though an irreversible decomposition of the radical was caused by ultraviolet light. For kinetic measurements, therefore, visible light ( $\lambda > 400$  nm) was used. Figure 1 shows the growth and decay curves of 1 at various temperatures. The decay was first order at temperatures above  $-40$  °C. This first-order decay is called "the slow step" in this paper. A two-step decay is observed at temperatures below  $-45$  °C, as shown in Figure 1b, with no change of the ESR spectral pattern during the decay. "The fast step" observable at low temperature was nearly approximated by second-order decay, as represented by Figure 1c. These kinetics indicate the existence of the short-lived intermediate in analogy with the case of the dimerization of 1-methyl-2-methoxycarbonylpyridinyl radical,<sup>3</sup> and the following scheme can be written:



where DI and D are dimeric intermediate and dimer, respectively.

We can treat the kinetics of two steps independently because their decay rates are substantially different from each other. The fast step is approximately second order in the temperature range  $-65$  to  $-93$  °C. Deviation from second-order behavior at higher temperatures, because of the back-reaction, required application of the reversible second- and first-order treatment. Reaction rate for the fast step  $k_1$ , can be represented by the treatment as follows:<sup>3</sup>

$$2k_1t = \frac{-1}{2[\bar{\text{R}}]} \ln \left( \frac{[\text{R}] - [\bar{\text{R}}]}{[\text{R}] + [\bar{\text{R}}]} \cdot \frac{[\text{R}]_0 - [\bar{\text{R}}]}{[\text{R}]_0 + [\bar{\text{R}}]} \right) \quad (1)$$



- 1 R = CH<sub>3</sub>  
2 R = CH<sub>2</sub>CH<sub>3</sub>  
3 R = CH(CH<sub>3</sub>)<sub>2</sub>

phenylpyridinyl (3) radicals were also examined as part of the mechanistic study.

Absolute rate constants and thermodynamic parameters were determined for the dimerizations and equilibria. It is proposed

- (1) Akiyama, K.; Kubota, S.; Ikegami, Y. *Chem. Lett.* **1981**, 469-472.  
(2) Hermolin, J.; Levin, M.; Ikegami, Y.; Sawayanagi, M.; Kosower, E. *M. J. Am. Chem. Soc.* **1981**, 103, 4795-4800.  
(3) Tero-Kubota, S.; Sano, Y.; Ikegami, Y. *J. Am. Chem. Soc.* **1982**, 104, 3711-3714.  
(4) Brown, G. H., Ed. "Techniques of Chemistry"; Wiley: New York, 1971; Vol. 3.

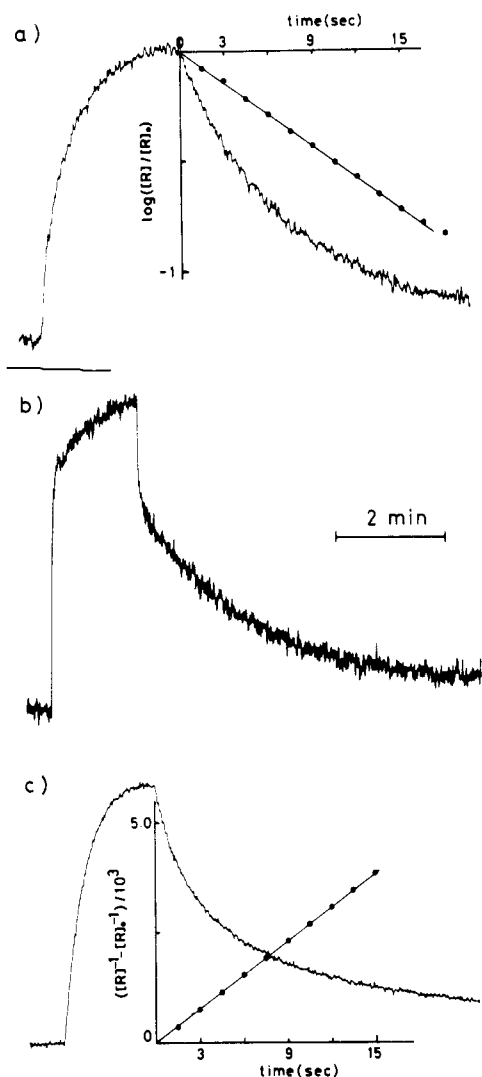


**Figure 1.** Growth and decay curves of 1-methyl-4-phenylpyridinyl radical in MTHF solution after a light pulse at (a)  $-10^{\circ}\text{C}$ , (b)  $-60^{\circ}\text{C}$ , and (c)  $-93^{\circ}\text{C}$ . Insert: (a) first-order plot and (c) second-order plot.

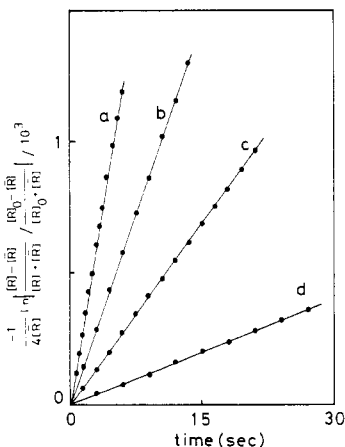


**Figure 2.** Reversible second- and first-order plots for the fast decay of the 1-methyl-4-phenylpyridinyl radical: (a)  $-65^{\circ}\text{C}$ , (b)  $-74^{\circ}\text{C}$ , (c)  $-84^{\circ}\text{C}$ , and (d)  $-93^{\circ}\text{C}$ .

where  $[R]$ ,  $[\bar{R}]$ , and  $[R]_0$  are the radical concentration, preequilibrium concentration, and initial concentration of the radical, respectively. In the derivation of eq 1, the condition,  $4K_1[\bar{R}] \gg 1$ , where  $K_1$  is preequilibrium constant, was used. As shown in Figure 2, very good linear relations were obtained for all measurements, indicating that the condition fit the present reaction. The Arrhenius plots were linear, yielding least-squares values for

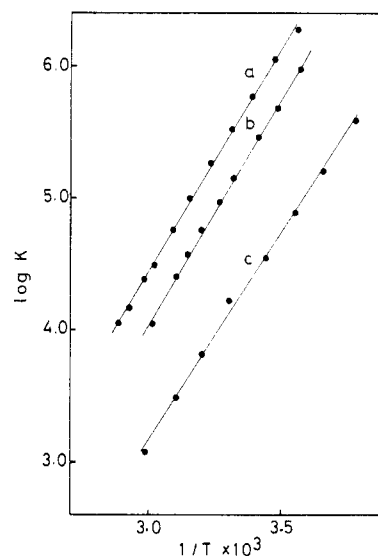


**Figure 3.** Monomer-dimer equilibrium constants ( $K = [D]/[R]^2$ ) vs.  $1/T$ : (a) 1-methyl-, (b) 1-ethyl-, and (c) 1-isopropyl-4-phenylpyridinyl radicals.

the activation energy ( $E_a$ ) of 6.65 kcal/mol and a frequency factor ( $A$ ) of  $1.95 \times 10^{10}$ . The rate constant of intermediate formation is  $2.77 \times 10^5 \text{ M}^{-1} \text{ s}^{-1}$  at room temperature, much smaller than that for a diffusion-controlled reaction.

The slow step of the radical decay was first order in the range  $-20$  to ca.  $65^{\circ}\text{C}$  (the reverse reaction can be neglected). The kinetic equation is represented as follows:

$$k_{\text{exp}} t = \frac{k_2}{2} t = -\ln \frac{[R] - [\bar{R}]}{[R]_0 - [\bar{R}]} \quad (2)$$

Arrhenius plots afforded  $E_a$  of 11.3 kcal/mol and a frequency factor of  $2.4 \times 10^8$ .

**Equilibrium Constant.** The total concentration of all species in a solution was determined by the quantitative titration with methyl viologen, which produces the methyl viologen cation radical ( $\epsilon$  13000 at 605 nm) by one-electron transfer from the pyridinyl radical.<sup>2</sup> Radical concentration was determined by using an electronic double integrator for ESR spectra. At temperatures above  $-20^{\circ}\text{C}$ , we can neglect the concentration of the intermediate in the determination of the equilibrium constant between the radical and the dimer, because the kinetic results suggest that its concentration is low. Therefore, the equilibrium constant can be obtained from the following equation:

$$K = \frac{[D]}{[R]^2} \approx \frac{[\text{total}] - [R]}{[R]^2}$$

where [total] is the total concentration of species containing in the system. Plots of  $\log K$  against  $1/T$  gave a good linear relation in the temperature range  $-20$  to  $65^{\circ}\text{C}$ , as shown in Figure 3. The changes of enthalpy and entropy involved in  $\sigma$ -bond formation between the pyridinyl radicals were  $\Delta H = -17.1$  kcal/mol and  $\Delta S = -31.8$  eu, respectively.

**1-Alkyl Group Size Effect.** As mentioned above, pyridinyl radical **1** dimerizes via a two-step process, just as in the case of 1-methyl-2-methoxycarbonylpyridinyl radical. However, the relatively high activation energy for the fast step,  $E_{a1} = 6.65$  kcal/mol, suggests that the intermediate of the dimerization process of **1** is a  $\sigma$ -bonding dimer rather than a  $\pi$  complex.<sup>5</sup> In order to clarify the dimerization pathway, the effect of 1-alkyl group size on the kinetic and thermodynamic parameters was examined.

(5) We tried to observe the absorption spectrum of the intermediate by the accumulation of its concentration by light irradiation at low temperature. The result showed that the intermediate has no absorption band at visible region. UV absorption measurements were not useful due to overlap of radical absorption with that of the dimer.

**Table I.** Activation Parameters for the Dimerization Reaction of 1-Alkyl-4-phenylpyridinyl Radicals

1-alkyl substituent	fast step			slow step		
	$k_1,^a \text{ M}^{-1} \text{ s}^{-1}$	$\log A,^b \text{ M}^{-1} \text{ s}^{-1}$	$E_a,^b \text{ kcal/mol}$	$k_2,^a \text{ s}^{-1}$	$\log A,^b \text{ s}^{-1}$	$E_a,^b \text{ kcal/mol}$
methyl	$2.77 \times 10^5$	$10.3 \pm 0.1$	$6.65 \pm 0.04$	1.31	$8.4 \pm 0.2$	$11.3 \pm 0.2$
ethyl	$2.28 \times 10^6$	$10.2 \pm 0.4$	$6.7 \pm 0.1$	0.586	$8.7 \pm 0.3$	$12.2 \pm 0.2$
isopropyl	$3.07 \times 10^4$	$9.4 \pm 0.3$	$6.7 \pm 0.1$	0.292	$9.2 \pm 0.5$	$13.3 \pm 0.3$

<sup>a</sup> Estimated at 300 K. <sup>b</sup> Error limits are standard deviations which do not reflect our real potential error caused by the measurements of time, temperature, and concentration.

**Table II.** Thermodynamic Parameters for the Monomer-Dimer Equilibria of 1-Alkyl-4-phenylpyridinyl Radicals ( $2\text{R}^\cdot \rightleftharpoons 2,2'\text{-Dimer}$ )

1-alkyl substituent	$\log K,^a \text{ M}^{-1}$	$\Delta H,^b \text{ kcal/mol}$	$\Delta S,^b \text{ eu}$	$\Delta G,^a,^b \text{ kcal/mol}$
methyl	5.52	$-17.1 \pm 0.1$	$-31.8 \pm 0.3$	$-7.6 \pm 0.1$
ethyl	5.08	$-17.0 \pm 0.1$	$-33.3 \pm 0.5$	$-7.0 \pm 0.2$
isopropyl	4.02	$-16.6 \pm 0.2$	$-36.9 \pm 0.6$	$-5.5 \pm 0.3$

<sup>a</sup> Estimated at 300 K. <sup>b</sup> See footnote b in Table I.

Kinetic measurements for 1-ethyl- (**2**) and 1-isopropyl-4-phenylpyridinyl (**3**) radicals afforded similar two-step decay processes. Reversible second- and first-order decay and first-order decay were observed for the fast and slow steps, respectively; the kinetic parameters are summarized in Table I. Rate constants for both steps were significantly affected by the 1-alkyl group and the fact that the frequency factor for intermediate formation depends on the size of the alkyl group, while the activation energy is constant within experimental error. On the other hand, in the slow step, both parameters are influenced by the size of the 1-alkyl group.

Equilibrium constants for **2** and **3** were also measured. The equilibrium moves toward the radical side with an increase in the size of 1-substituent. A good linear relation between  $\log K$  and  $1/T$  was obtained for both **2** and **3** in the temperature range  $-20$  to  $65^\circ \text{C}$ , as shown in Figure 3. The thermodynamic parameters measured are listed in Table II. The data show that the 1-alkyl group size effect on dimer formation is mainly due to the entropy term.

**Structure of the Diamagnetic Dimer, D.** Since the monomer-dimer equilibrium of **1** lies largely on the side of the dimer at low temperature, a relatively broad but analyzable  $^1\text{H}$  NMR spectrum of the diamagnetic dimer could be obtained below  $-50^\circ \text{C}$ . Broadening is probably caused by a small amount of the radical monomer. Absorption lines were observed at  $\delta$  (ppm) 3.4 (6 H), 4.0–4.3 (2 H), 5.3–5.5 (2 H), 5.5–5.9 (2 H), 6.3–6.5 (2 H), and 6.9–7.8 (10 H) in  $\text{THF}-d_8$ ,  $\delta(\text{Me}_4\text{Si})$  0.00. This NMR spectrum indicates that all of the protons in each pyridine ring of the dimer are nonequivalent to each other. It is thus concluded that the diamagnetic dimer is the 2,2'-dimer, supported by agreement of the  $\delta$  values with those of the 2,2'-dimer of 1-trimethylsilyl-4-phenylpyridinyl radical.<sup>6</sup> Additional NMR lines were also observed in the present measurement, though these could not be analyzed because of overlap with the main absorptions. NMR measurement for the solutions of **2** and **3** has been unsuccessful.

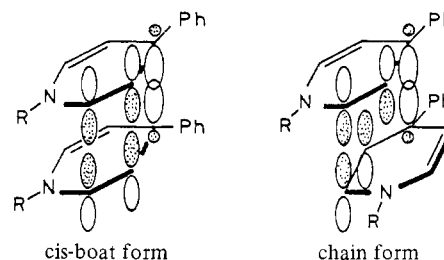
## Discussion

**Dimerization Mechanism.** As shown in Table I,  $E_{a1} = 6.7$  kcal/mol was obtained irrespective of the size of 1-alkyl group. This relatively large  $E_a$  value implies that the intermediate is a  $\sigma$ -bonding dimer, with the ring-ring bond distant from the 1-alkyl group. Since free radicals are apt to react at positions with high spin density and the spin density is large at the 4-position (Table III), the 4,4'-dimer is the most probable structure for the  $\sigma$ -bonded intermediate. This dimer might also be expected from a plausible structure for the dimeric  $\pi$  complexes.<sup>7,8</sup> The  $\pi$  complex expected from 4-phenylpyridinyls would have the stacked structure with

**Table III.** Experimental and Calculated Spin Densities of **1**

position	$\rho_{\text{exptl}}^a$	$\rho_{\text{calcd}}^b$	SOMO coeff
1	0.133	0.201	-0.443
2, 6	0.158	0.223	0.421
3, 5	(-)0.0364	-0.0570	0.149
4		0.301	-0.480
7		0.00128	-0.135
8, 12	0.103	0.0663	0.219
9, 11	(-)0.0176	-0.0221	0.0473
10	0.129	0.0788	-0.238

<sup>a</sup>  $Q_{\text{CH}}^{\text{H}} = -26.1$ ,  $Q_{\text{CN}}^{\text{N}} = 9.1$ , and  $Q^{\text{N}} = 15.6 \text{ G}$ .<sup>11</sup> <sup>b</sup> Parameters for the McLachlan calculation. Coulomb integral ( $\alpha_{\text{X}} = \alpha_0 + h_{\text{X}}\beta_0$ ):  $h_1 = 1.5$ ;  $\delta h_2 = \delta h_6 = 0.3$ . Resonance integral ( $\beta_{\text{CX}} = k_{\text{CX}}\beta_0$ ):  $k_{1,2} = k_{1,6} = 1.0$ ;  $k_{4,7} = 0.9$ .

**Scheme I**

a head-to-tail configuration, in which both 4-positions in two stacked pyridinyl radicals are close each other enough to couple readily to form a  $\sigma$  bond. Thus, the  $\pi$  complex formation leads to lowering the activation energy in the dimerization process.

The 4,4'-dimer formed is able to have the configuration involving 1,5-hexadiene system between two pyridine rings, which is constructed by the 2–3 and 5'–6' double bonds for chair form, and the 2–3 and 2'–3' bonds for cis-boat form by the rotation about the 4–4' bond as depicted in Scheme I. The shaded and unshaded regions correspond to the plus and minus lobes of the singly occupied MO's (SOMO's) for the pyridinyl radicals. These systems are liable to induce the thermal [3,3] sigmatropic rearrangement<sup>9</sup> since the phases of MO's coincide at the 2- and 6'-positions in the chair form and at the 2- and 2'-positions in the cis-boat form, respectively. Thus, the rearrangement is symmetry allowed, as treated by the frontier-orbital method,<sup>10</sup> and accessible, moreover, because these positions hold high spin densities in SOMO (Table III). The chair form gives the 2,6'-dimer and the cis-boat form produces the 2,2'-dimer, respectively. They are diastereoisomers of each other. The production of 2,2'-dimer or the 2,6'-dimer of **1** was confirmed by the NMR spectrum, which shows that the covalent bond is formed between pyridine rings, rather than between the phenyl-phenyl or phenyl-pyridine rings, and the protons in the pyridine ring are magnetically nonequivalent to each other. Thus, Scheme II can be proposed as the dimerization process for **1**.

The fast step is 4,4'-dimer formation, in which  $\pi$ -complex formation may participate. The slow step is Cope rearrangement from the 4,4'-dimer to the 2,2'- or/and 2,6'-dimer. These two products are diastereoisomers of each other, with the 2,2'-dimer

(6) Neumann, W. P.; Reuter, K. *Chem. Ber.* **1979**, *112*, 936–949.

(7) Itoh, M.; Nagakura, S. *J. Am. Chem. Soc.* **1967**, *89*, 3959–3965.

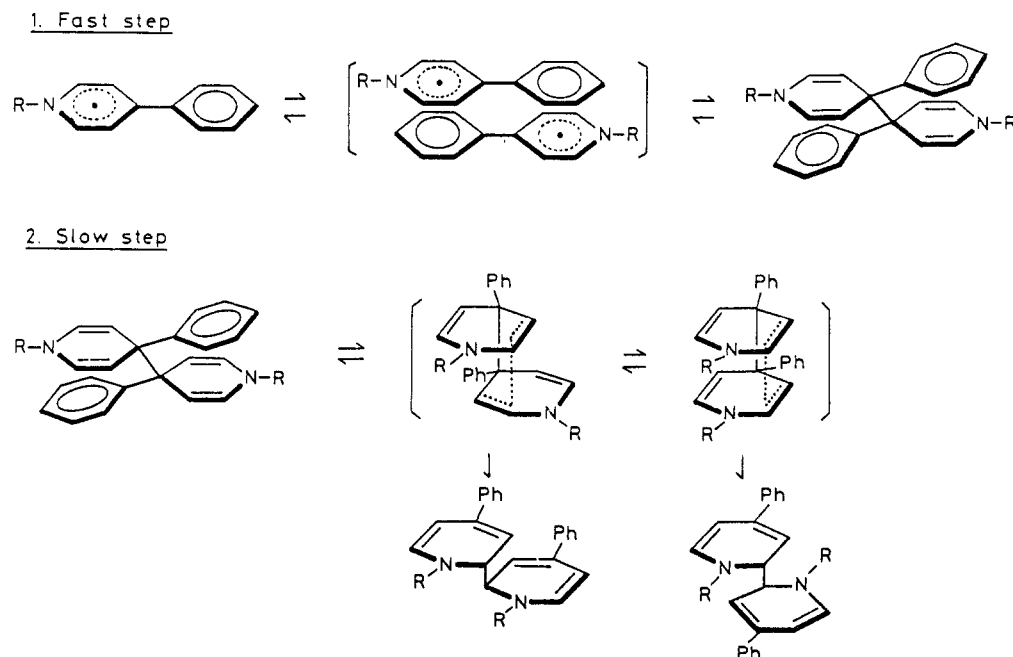
(8) Ikegami, Y.; Kubota, S.; Watanabe, H. *Bull. Chem. Soc. Jpn.* **1979**, *52*, 1563–1567.

(9) Rhoads, S. J. In "Molecular Rearrangements"; de Mayo, P., Ed.; Wiley: New York, 1963; Part 1, pp 655–706.

(10) Fukui, K. *Acc. Chem. Res.* **1971**, *4*, 57–64.

(11) Zeldes, H.; Livingston, R. *J. Phys. Chem.* **1973**, *77*, 2076–2081.

Scheme II



corresponding to the meso form and the 2,6'-dimer to the racemic compound.

Either of the two kinds of dimers may be produced since only one reaction path was kinetically measured in the slow step at temperatures above  $-40^{\circ}\text{C}$ . The activation energies of the chair and cis-boat forms should be distinct because of the difference of the molecular orbital interaction and steric hindrance. On the assumption that both **2** and **3** dimerize in a similar way as above, the observed size effect of the 1-alkyl group on  $k_2$  indicates a kinetic preference for 2,2'-dimer formation. The formation of the cis-boat form is significantly influenced by the 1-alkyl group while steric hindrance is small in chair form. The observed kinetic parameters  $E_a$  and  $A$  term in the slow step significantly depend on the bulkiness of the 1-alkyl group, as shown in Table I. Thus, the present results strongly imply that the slow step corresponds to the 2,2'-dimer formation process via the cis-boat form from the 4,4'-dimer by sigmatropic rearrangement.

**Kinetic and Thermodynamic Parameters for the Dimerization.** The rate constant of the fast step of **1** at  $27^{\circ}\text{C}$  is  $2.77 \times 10^5 \text{ M}^{-1} \text{ s}^{-1}$ . This value is 4 or 5 orders of magnitude smaller than that of a diffusion-controlled reaction. This is ascribed to the relatively high  $E_a$  (6.7 kcal/mol) and low  $A$  ( $2.0 \times 10^{10}$ ) values. These kinetic parameters are appropriate for  $\sigma$ -bond formation between the radicals stabilized by spin delocalization. The activation energies for **1**–**3** are comparable to those for the dimerization reactions of triphenylmethyl (6.95 kcal/mol)<sup>12</sup> and 2,4,5-triphenylimidazolyl (7.4 kcal/mol)<sup>13</sup> radicals. The covalent bond formation between the 4,4'-positions of **1**–**3** would be affected by the bulky phenyl group. This steric effect is probably compensated by  $\pi$ -complex formation participating in the transition state. The observed frequency factors of the fast step ( $2.0 \times 10^{10}$  to  $2.4 \times 10^9$ ) are larger than those of the dimerization of triphenylmethyl ( $3.9 \times 10^7$ ) and 2,4,5-triphenylimidazolyl ( $1.7 \times 10^7$ ). This may be due to  $\pi$ -complex formation in the present dimerization.

As mentioned above, [3,3] sigmatropic rearrangement was proposed for the slow step. The intramolecular rearrangement is one of the most interesting fields for the theorists and experimentalists. Many kinetic studies for the rearrangement reactions

have been carried out and the wide variety of activation energy values, for example, 5.3 kcal/mol for semibulvalene<sup>14</sup> and 40 kcal/mol for hexadienyl,<sup>15</sup> have been reported. However, there are few works on the rearrangement of the systems consisted of conjugated rings containing nitrogen atoms.

The cis-boat form in the transition state proposed in this work is similar to that of benzidine rearrangement reported by Shine et al.<sup>16</sup> in which a [5,5] sigmatropic rearrangement occurs. They preferred a concerted mechanism in order to explain kinetic isotope effects. Pyridinyl radicals may play an important role to investigate the factors governing the concerted reactions, because various derivatives can be prepared in pure state. Two examples of the rearrangements have been reported for a 4,4'-dimer of 1-(ethoxycarbonyl)-4-methylpyridinyl<sup>17</sup> and a 2,4'-dimer of 3,5-(diethoxycarbonyl)-1,2,6-trimethylpyridinyl,<sup>18</sup> yielding more stable dimers, 2,2'-dimer and 4,4'-dimer, respectively.

The enthalpy changes accompanied with the dimer formations were  $-17.1$ ,  $-17.0$ , and  $-16.6$  kcal/mol for **1**, **2**, and **3**, respectively. These values are comparable to those for C–C bond formation in the dimerizations of 2-substituted pyridinyls<sup>3</sup> and some phenoxy radicals.<sup>19</sup> Two pyridine rings can be planar in the dimer and are located probably in the configuration of the least steric hindrance of each other. This reflected in the result that entropy terms are significantly influenced by the steric effect of the 1-alkyl group though there is little change in the enthalpy difference.

**Acknowledgment.** We are grateful to Dr. Tsutomu Miyashi of the Faculty of Science in this University for his helpful discussions.

**Registry No.** **1**, 85304-48-9; **1** dimer, 85269-21-2; **2**, 85304-47-8; **3**, 85304-49-0.

(14) Cheng, A. K.; Anet, F. A. L.; Mioduski, J.; Meinwald, J. *J. Am. Chem. Soc.* **1974**, *96*, 2887–2891.

(15) Doering, W. v. E.; Toscano, V. G.; Beasley, G. H. *Tetrahedron* **1971**, *27*, 5299–5306.

(16) Shine, H. J.; Zmuda, H.; Park, K. H.; Kwart, H.; Horgan, A. G.; Brechbiel, M. *J. Am. Chem. Soc.* **1982**, *104*, 2501–2509.

(17) Atlani, P.; Biellmann, J. F.; Briere, R.; Rassat, A. *Tetrahedron* **1972**, *28*, 5805–5822.

(18) McNamara, F. T.; Niefert, J. W.; Ambrose, J. F.; Huyser, E. S. *J. Org. Chem.* **1977**, *42*, 988–993.

(19) Mahoney, L. R.; Weiner, S. A. *J. Am. Chem. Soc.* **1972**, *94*, 585–590.

(12) D'yachkovskii, F. S.; Bubnov, N. N.; Shilov, A. E. *Dokl. Akad. Nauk SSSR* **1958**, *122*, 629–631.

(13) Maeda, K.; Hayashi, T. *Bull. Chem. Soc. Jpn.* **1970**, *43*, 429–438.